Science of Advanced Materials
Vol. 4, pp. 351–365, 2012
(www.aspbs.com/sam)

ARTICLE

Influence of Gas Pressure in Radio Frequency Sputtering on Microstructure and Optical Properties of VO_2(M) Thin Films

Y. H. Tian, S. S. Pan, Y. Y. Luo, and G. H. Li*

Key Laboratory of Materials Physics, Anhui Key Laboratory of Nanomaterials and Nanotechnology, Institute of Solid State Physics, Chinese Academy of Sciences, Hefei 230031, P.R. China

ABSTRACT

VO_2(M) thin films have been grown by radio frequency reactive magnetron sputtering under different gas pressures. The microstructure and optical constants of the films were investigated. It was found that the grain size of VO_2 in the film increases and the deposition rate decreases with increasing deposition gas pressure. The refractive index and reflectivity in near-infrared wavelengths range and the optical band gap increases with increasing gas pressure.

KEYWORDS: VO_2, Optical Properties, Sputtering, Ellipsometry, Gas Pressure.

1. INTRODUCTION

The monoclinic phase vanadium dioxide (VO_2(M)) have attracted much attention due to its insulator-to-metal phase transition phenomena.[1] The VO_2(M), as semiconductor with a narrow band gap (670 meV) at room temperature, can be induced the structural phase transition to rectangular crystalline by light excitation[1–3] or thermally at a temperature of 340 K. The optical and electrical characters, such as transmittance, reflectivity and refractive constant and conductivity, will change distinctly. Due to the repeatable, reversible and rapidly phase transition properties, VO_2(M) is considered as a promising candidate for thermal excitation electronic and optical devices, such as heat detection[4–6] and energy saving coatings,[7–10] laser protector,[11,12] modulation and polarization[13] devices in sub-micron wavelength.

The semiconductor to metal phase transition (SMT) and optical properties depend strongly on the grain size and thickness of VO_2(M) thin films,[3,14–16] and the nucleation of the metallic phase is considered to be a critical factor in deterring the formation of a metastable state in VO_2. Magnetron sputtering technique is a widely used method to grow high quality thin films. The vanadium ion has several valence states, such as +3, +4, +5, and the formation of M-phase VO_2 is very sensitive to the sputtering conditions, such as substrate temperature,[17] oxygen concentration[18–20] substrate bias effect[21] and boundary layer.[22,23] In this paper, we report the influence of sputtering gas pressure on the microstructure and optical properties of VO_2 films, and it was found not only the grain size and growth rate, but also the optical band gap and the optical constants depend strongly on gas pressure.

*Author to whom correspondence should be addressed.
Email: ghli@issp.ac.cn
Received: 19 May 2011
Accepted: 20 May 2011

2. EXPERIMENTAL DETAILS

The VO_2(M) thin films were deposited on *n*-Si(100) wafer by radio frequency magnetron sputtering technique with a power of 300 W. The base pressure of the deposition chamber was around 5.0×10^{-4} Pa or better. The vanadium target (purity: 99.999%) and the gas mixture of high purity argon (purity: 99.999%) and oxygen (purity: 99.999%) was used as sputtering source and working gas. The gas flow rate of oxygen and argon was 0.6 and 49.4 SCCM, respectively. The sputtering gas pressure, P_{gas}, of chamber was maintaining by airlock and changed from 0.1 to 0.35 Pa. The substrate temperature was maintained at 500 °C during sputtering and cooled to room temperature spontaneously after 40 mins deposition.

Crystal structure of the as-prepared thin films were analyzed by grazing angle X-ray diffraction (XRD) achieved with a Philips X'Pert Pro MPD diffractometer, using Cu-Kα radiation with a wavelength of 1.5406 Å. Surface morphology and thickness of films was observed using Sirion 200 field emission scan electron microscopy (FESEM) operating with an accelerating voltage of 5 kV. Optical constants were analyzed using an *ex situ* phase modulated spectroscopic ellipsometry (Model UVISEL

Jobin-Yvon) over the spectral range of 0.75–6.5 eV at 70° incidence angle. The optical reflection spectra were obtained by spectrometer (Shimadzu UV 3600) in the wavelength range of 500–2500 nm.

3. RESULTS AND DISCUSSION

3.1. The Morphology and Crystal Structure

The XRD patterns of VO_2 films with different sputtering gas pressures are presented in Figure 1. One can see that all the diffraction peaks can be well indexed to M-phase VO_2 (JPCDS card No. 44-0252) and no other phases can be detected, indicating that the films prepared at different gas pressures are all the M-phase VO_2. The crystallite size in the growth direction, D, can be estimated from XRD patterns using the Scherrer relationship: $D = 0.94\lambda/\beta\cos\theta$, where β is the full width at half maximum of a diffraction peak at 2θ corrected for instrumental broadening, and the average VO_2 crystallite size in the films is found to be about 27, 24 and 16 nm with gas pressure of 0.35, 0.2 and 0.1 Pa, respectively.

Figure 2 shows the FESEM images of the VO_2 films grown under different gas pressures. One can see that the average particle size decreases with decreasing P_{gas} and is in the range of 30∼70 nm, which is larger than that obtained by XRD analysis, indicating that the VO_2 particles are the agglomeration of small nanocrystals. The films thickness (from the section views of the films, the images are not shown here) is about 105, 115 and 140 nm for the gas pressure of 0.35, 0.2 and 0.1 Pa, respectively. Considering the growth time of 40 minutes, the corresponding growth rate of the film is about 2.62, 2.88 and 3.5 nm/min for the gas pressure of 0.35, 0.2 and 0.1 Pa, respectively. These results indicate that the particle size decreases but growth rate of the VO_2 film increases with decreasing P_{gas}, and the crystal structure of VO_2 film is stable upon gas pressure varying. Due to high argon partial pressure of 99.2%, the Ar ion is the dominant sputtering ions. The high gas pressure will induce a larger amount of argon atoms/ions in the reactor chamber, which will effectively increase the collision rates of vanadium atoms sputtered from the target with atomic/ionic oxygen, leading to the decrease of the growth rate, and thus the reduced thickness of the thin film.

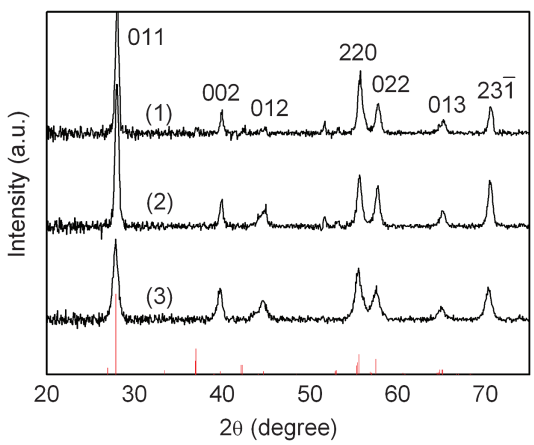

Fig. 1. XRD patterns of VO_2 films sputtered at gas pressure of (1) 0.35, (2) 0.2 and (3) 0.1 Pa.

3.2. Optical Constants

The optical constants of the VO_2 films have been investigated by SE. SE is a sensitive, powerful and nondestructive method to characterize the linear optical response of thin film. Based on the microstructure characterization and ellipsometry measurement of the VO_2 films, a two-layer model on Si(100) substrate was built to simulate the VO_2 films: homogeneous VO_2 layer, and surface layer consisting of void and VO_2 based on the Bruggeman effective medium approximation, as shown schematically in the inset of Figure 2(b). The Tauc-Lorentz (TL) dispersion model was used to describe the optical dielectric function (ε) of the VO_2 films, as expressed by following equations:

$$\varepsilon_i(E) = \begin{cases} \dfrac{AE_0C(E-E_g)^2}{(E^2-E_0^2)^2+C^2E^2}\dfrac{1}{E} & (E > E_g) \\ 0 & (E \le E_g) \end{cases} \quad (1)$$

$$\varepsilon_r(E) = \varepsilon_\infty + \frac{2}{\pi}P\int_{E_g}^{\infty}\frac{\xi\varepsilon_i(\xi)}{\xi^2-E^2}\,d\xi \quad (2)$$

Meanwhile, the optical constants (n, k) are determined as follow:

$$n = \frac{1}{\sqrt{2}}\sqrt{\varepsilon_r+\sqrt{\varepsilon_r^2+\varepsilon_i^2}} \quad \text{and} \quad k = \frac{1}{\sqrt{2}}\sqrt{-\varepsilon_r+\sqrt{\varepsilon_r^2+\varepsilon_i^2}} \quad (3)$$

The TL model combined quantum mechanical approach and classical Lorentz oscillator model. The imaginary part $\varepsilon_i(E)$ of the TL dielectric function in Eq. (1) contains four parameters: E_g (band gap), E_0 (peak transition energy), C (broadening parameter) and A (transition matrix element). The real part $\varepsilon_r(E)$ in Eq. (2) is obtained by performing a Kramers-Kronig integration of $\varepsilon_i(E)$, and here P in Eq. (2) stands for the Cauchy principal part of the integral. The thickness and the optical dielectric constants were extracted based on the best fit (χ^2: goodness of fit) in the least-squares fit procedure between experimental SE data and the simulated one. The volume fraction of void in surface layer, f, the variable in the fitting calculation, is defined by the following equation:

$$f = \frac{V_{void}}{V_{void}+V_{VO_2}} \quad (4)$$

where V_{void} and V_{VO_2} denote void and VO_2 volume in surface layer, respectively.

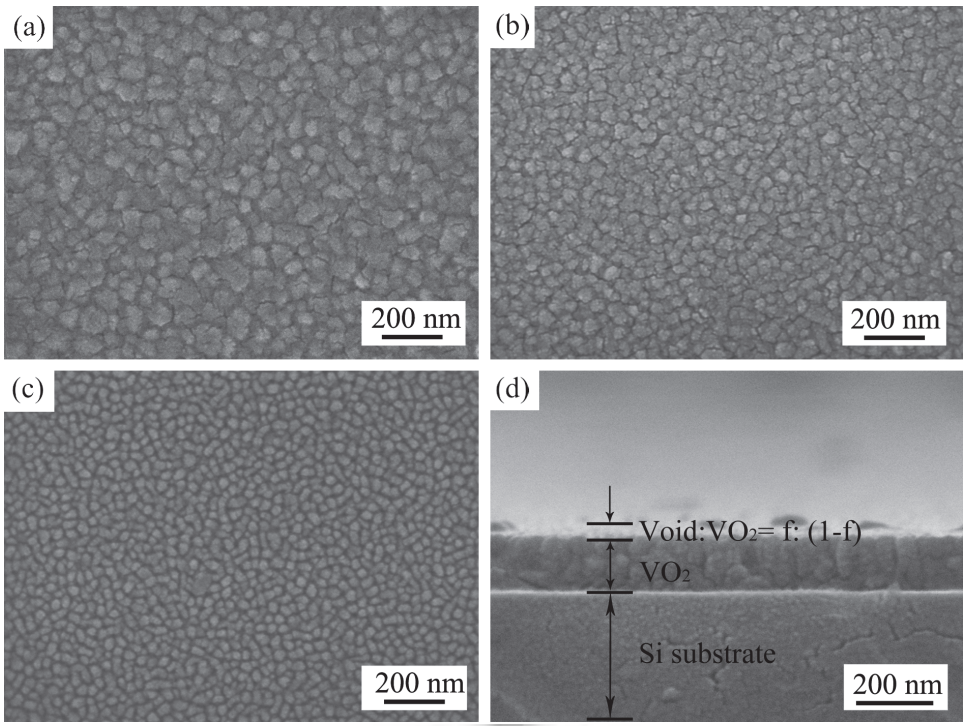

Fig. 2. SEM images of VO_2 films sputtered at gas pressure of (a) 0.35, (b) 0.2 and (c) 0.1 Pa; (d) cross-sectional SEM image and (c) and the two-layer model in SE simulation.

Figure 3 shows the experimental (points) and fitted (lines) SE data of Δ and Ψ (measurement parameter of ellipsometry) of the VO_2 films with different gas pressures. One can see that the spectra for these three films have similar features. The simulated curves agree well with the experimental data, and hence the material property can be described accurately. Based on the simplified two-phase model, the best fitting results are listed in Table I. From this table one can see that the thickness of VO_2 film (surface layer plus VO_2 layer) increases with decreasing P_{gas} and is consistent with the SEM result. The void ratio of surface layer, the inverse proportion to the packing density, decreases with decreasing P_{gas}. From Table I one also can see that optical band gap E_g obtained from the fitting result is about 0.606, 0.469 and 0. 456 eV for 0.35, 0.2 and 0.1 Pa, respectively, which is lower than E_g of the single crystalline[3] due to the contribution of quantum size effect of the present VO_2 thin film. On the other hand, however, the optical band gap of VO_2 thin films decreases from 0.606 to 0.456 eV with decreasing P_{gas}, while the VO_2 crystal size decreases with decreasing P_{gas}, an obvious redshift of the optical band gap was found with the decreased grain size. This kind of redshift has been observed in literatures[24] and is considered mainly attributed to the relaxation of the induced compressive stress in the films.[25] In present case of sputtering deposition, this intrinsic stress arises due to the bombardment of the energetic species. The films deposited at lower gas pressure will exhibit a compressive stress. In the sputtering process, the highly energetic species could be implanted below the VO_2 surface, which is likely to induce high intrinsic stresses by creating the defects. For the VO_2 thin film grown at high gas pressure, the strain could quickly relaxed due to the high kinetic energy, and leads to the increase in band gap.

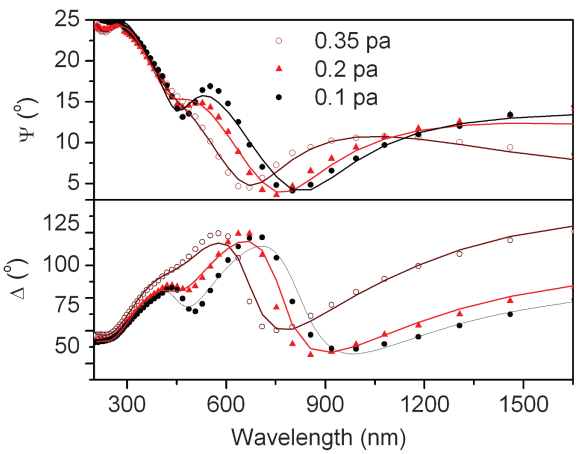

Fig. 3. The experimental (points) and fitted (lines) data of Δ and Ψ of the VO_2 film sputtered at different gas pressures.

There exists a relationship between the extinction coefficient and absorption coefficient: $\alpha = 4\pi k/\lambda$, and the absorption coefficient α is connected with the optical band gap energy E_g^* by the equation $\alpha^\eta \propto (h\nu - E_g^*)$, the index η characterizes the optical absorption process and is

ARTICLE

Table I. Characters of VO_2 films extracted from the best simulation results using Tauc-Lorentz model with different sputter gas pressure P_{gas}.

$P_{gas}(Pa)$	VO_2 layer thickness (nm)	Surface layer thickness (nm)	Total thickness (nm)	f (%)	E_g (eV)	$E_g*(eV)$	n@1500 nm	χ^2
0.35	89.0	16.1	106.1	77.2	0.606	0.75	3.17	1.1
0.2	109.5	16.3	125.8	63.7	0.469	0.61	2.84	2.71
0.1	123.5	18.0	141.5	58.8	0.456	0.55	2.72	3.96

theoretically equal to 1/2 and 2 for indirect allowed and direct allowed transitions, respectively. The value of E_g^* can be obtained by the intercept on the $h\nu$ axis in the plot of $(\alpha h\nu)^\eta$ versus $h\nu$. It was found the best plot was obtained for the direct allowed transitions and the results for E_g^* are also listed in Table I. The obtained result also shows that the optical band gap VO_2 film increases with increasing P_{gas} and approximates to the E_g values extracted from TL model in SE simulation.

Figure 4(a) shows the refractive index (n) and extinction coefficient (k) of the VO_2 films calculated from the extracted best-fitted parameters. One can see that the refractive index slightly decreases in visible light region and is close to a constant of about 3. Beyond visible light region the refractive index depends strongly on P_{gas}, and firstly increases slightly and decreases again at wavelength higher than 800 nm for the film prepared at lower pressure of 0.35 Pa, while for the film prepared at lower pressure of 0.2 Pa, the refractive index slightly increasing at wavelength higher than 1200 nm, and for the film prepared at lower pressure of 0.1 Pa the refractive index always decreases with wavelength. From Figure 4(a) one can see that the refractive index in near-infrared wavelengths range decreases with decreasing gas pressure. In general, the packing density is the mainly factor of refractive index, and the lower the packing density the lower the refractive index. While in present case the packing density increases with decreasing P_{gas}, see Table I, and thus other factors will affect the refractive index. The collision rates of vanadium atoms sputtered from the target with atomic/ionic oxygen will be low under low deposition gas pressure, and the corresponding deposition rate of VO_2 film will increases, as mentioned above, the growth rate is 3.5 nm/min for the gas pressure 0.1 Pa compared to the 2.62 nm/min for the 0.35 Pa. The sputtering atoms hardly have enough time to migrate to the lowest energy equilibrium position, resulting in the formation of a large amount of defects, such as oxygen vacancies, and thus leading to the decrease in the refractive index with decreasing gas pressure. Figure 4(b) shows the extinction coefficient of VO_2 films. The extinction coefficient is close to 0.4 from 400 and 1200 nm, and decreases with increasing P_{gas} at wavelength larger than 1200 nm.

3.3. Reflectance Spectrum

Figure 5(a) shows the reflective spectra of VO_2 films measured from the spectrometer. One can see that the average reflectivity is about 65% and slightly decreases with wavelength from 400 to 1900 nm, and increases with increasing P_{gas}. A similar result can be obtained from SE simulation, as shown in Figure 5(b). The relative lower reflectivity obtained from SE simulation is due to the fact that only the reflective light at the angle of incidence 70° was collected. The increased reflectivity is considered due to the increased VO_2 grain size with increasing gas pressure.

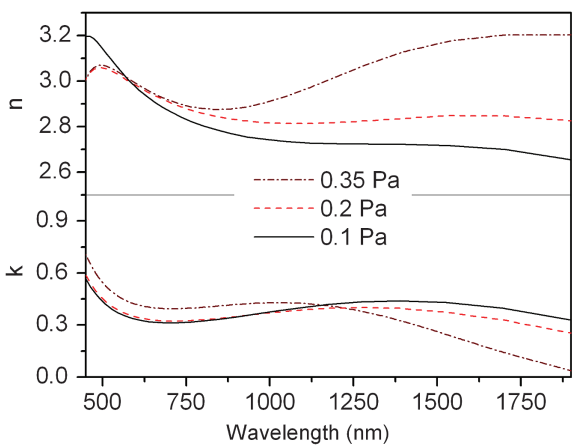

Fig. 4. Calculated refractive index (n) and extinction coefficient (k) of VO_2 thin films sputtered at different gas pressures.

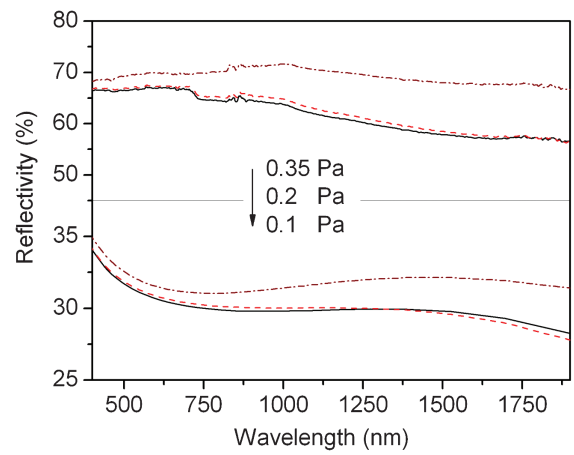

Fig. 5. Reflective spectra of VO_2 films sputtered at different gas pressures from (a) spectrometer and (b) SE simulation.

4. CONCLUSION

VO_2 thin films have been grown on Si(100) substrates by radio frequency reactive magnetron sputtering. The film thickness decreases and grain size of the VO_2 films increases with increasing sputtering gas pressure. The refractive index and reflectivity in the near-infrared wavelengths and the optical band gap increases with increasing sputtering gas pressure, the increased refractive index is due to defect effect, while the increased optical band gap is considered mainly attributed to the relaxation of induced compressive stress in the films.

Acknowledgments: This work was financially supported by the National Basic Research Program of China (2009CB939903) and the National Natural Science Foundation of China (Grant number: 11004197, 11104270).

References and Notes

1. F. J. Morin, *Phys. Rev. Lett.* 3, 34 **(1959)**.
2. R. M. W. M. F. Becker, A. B. Buckman, P. Georges, and A. Brun, *Appl. Phys. Lett.* 65, 1507 **(1994)**.
3. M. Rini, Z. Hao, R. W. Schoenlein, C. Giannetti, F. Parmigiani, S. Fourmaux, J. C. Kieffer, A. Fujimori, M. Onoda, S. Wall, and A. Cavalleri, *Appl. Phys. Lett.* 92, 181904 **(2008)**.
4. L. Kang, Y. Gao, Z. Chen, J. Du, Z. Zhang, and H. Luo, *Sol. Energy Mater. Sol. Cells* 94, 2078 **(2010)**.
5. J. Lappalainen, *Sens. Actuators A: Physical* 142, 250 **(2008)**.
6. S. Chen, *Sens. Actuators A: Physical* 115, 28 **(2004)**.
7. H. Kakiuchida, P. Jin, S. Nakao, and M. Tazawa, *Jpn. J. Appl. Phys.* 46, L113 **(2007)**.
8. R. Balu and P. V. Ashrit, *Appl. Phys. Lett.* 92, 021904 **(2008)**.
9. J. B. K. Kana, J. M. Ndjaka, B. D. Ngom, A. Y. Fasasi, O. Nemraoui, R. Nemutudi, D. Knoesen, and M. Maaza, *Opt. Mater.* 32, 739 **(2010)**.
10. A. Romanyuk, R. Steiner, L. Marot, and P. Oelhafen, *Sol. Energy Mater. Sol. Cells* 91, 1831 **(2007)**.
11. A. Ilinski, *J. Non-Cryst. Solids* 338, 266 **(2004)**.
12. E. V. Babkin, A. P. Dolgarev, and H. O. Urinov, *Thin Solid Films* 150, 4 **(1987)**.
13. J. C. C. F. Fan, R. Harold, Bachner, and J. Frank, *Appl. Phys. Lett.* 31, 11 **(1977)**.
14. D. Brassard, S. Fourmaux, M. Jean-Jacques, J. C. Kieffer, and M. A. El Khakani, *Appl. Phys. Lett.* 87, 051910 **(2005)**.
15. G. Xu, P. Jin, M. Tazawa, and K. Yoshimura, *Appl. Surf. Sci.* 244, 449 **(2005)**.
16. S. Lysenko, V. Vikhnin, A. Rúa, F. Fernández, and H. Liu, *Phys. Rev. B* 82, 205425 **(2010)**.
17. A. Gentle, A. Maaroof, and G. Smith, *Curr. Appl. Phys.* 8, 229 **(2008)**.
18. J. Lee, S. Min, H. Cho, and C. Chung, *Thin Solid Films* 515, 7740 **(2007)**.
19. T. W. Chiu, K. Tonooka, and N. Kikuchi, *Thin Solid Films* 518, 7441 **(2010)**.
20. C. H. Griffiths and H. K. Eastwood, *J. Appl. Phys.* 45, 2201 **(1974)**.
21. H. Miyazaki and I. Yasui, *J. Phys. D: Appl. Phys.* 39, 2220 **(2006)**.
22. F. B. Dejene and R. O. Ocaya, *Curr. Appl. Phys.* 10, 508 **(2010)**.
23. H. Kakiuchida, P. Jin, and M. Tazawa, *Int. J. Thermophys.* 31, 1964 **(2009)**.
24. B. A. Nejand, S. Sanjabi, and V. Ahmadi, *Vacuum* 85, 400 **(2010)**.
25. R. Kumar, N. Kharec, V. Kumara, and G. L. Bhallab, *Appl. Surf. Sci.* 254, 6509 **(2008)**.

ARTICLE